IMEKO 23rd TC3, 13th TC5 and 4th TC22 International Conference
30 May to 1 June, 2017, Helsinki, Finland

PICO-METER METROLOGY FOR THE PRIMARY VIBRATION CALIBRATION

Wan-Sup Cheung and *Kyungmin Baik*

KRISS, Republic of Korea, wansup@kriss.re.kr

Abstract: This paper introduces the use of a homodyne differential plane mirror interferometer (HDPMI) for development of the primary vibration calibration system. The zero-drift test results showed that it enables displacement measurement in a scale of 10 pico-meters could be feasible. The HDPMI model was shown to be quite successful for the primary vibration calibration even in the frequency range of 5 kHz to 20 kHz. The standard uncertainty of the complex sensitivities from 5 kHz to 20 kHz was to be less than 0.46 % for their moduli and 0.57° for the phase shifts.

Keywords: Vibration, Primary calibration, laser interferometer, pico-meter metrology

1. INTRODUCTION

The displacement amplitude of 100 m/s^2-peak vibration at 10 kHz is equivalent to 4 % of a He-Ne laser wavelength. As the calibration frequency goes to 20 kHz, it decreases to 1 % of the laser wavelength. Here is an open question: how to realize a measurement uncertainty of 0.5 % or less even for such nano-meter (nm) amplitude vibration displacement. On the onset of this work, it became apparent that such challenging measurement uncertainty cannot be achieved without realizing the measurement resolution of pico-meters (pico-meter metrology).

In this work, a commercialized homodyne differential plane mirror interferometer (HDPMI) was selected to examine displacement measurement resolution-related issues. The measurement principle and uncertainty models of the select HDPMI model are represented in Section 2. To illustrate what amount of the measurement resolution of the HDPMI model can provide, the "zero-drift" test results are provided. They indicate that the background (bottom) noise level of the select HDPMI model was realised in this work.

A next generation model of the primary vibration calibration system recently set up in KRISS is introduced Section 3. It is target to extend the frequency range of vibration calibration up to 20 kHz (or higher, if possible). Including the select HDPMI setup introduced in Section 2, a new linear vibration exciter, the 12-bit digital scope and other instruments were integrated to the new primary vibration calibration system that is still under development. Preliminary calibration results in the frequency range of 5 kHz to 20 kHz using the new primary calibration system are demonstrated in this paper.

In Section 4, main contributions of this work are summarised and concluding remarks are finally made.

2. DISPLECEMENT MEASUREMENT LASER INTERFEROMETER

2.1 Homodyne Differential Plane Mirror Interferometer

Fig. 1 shows the commercialised homodyne differential plane mirror interferometer (HDPMI) used in this work. The Renishaw's HDPMI model, which consists of Renishaw RLE20 and RLD10-A3-P0, was chosen to measure vibration displacement. The optic configuration of the differential plane mirror interferometer has been most widely used in the length metrology since it enables one-dimension length measurement without effect of the unwanted angular motion of a moving target (or mirror) by using the dual measurement beams reflected from the plain mirror.

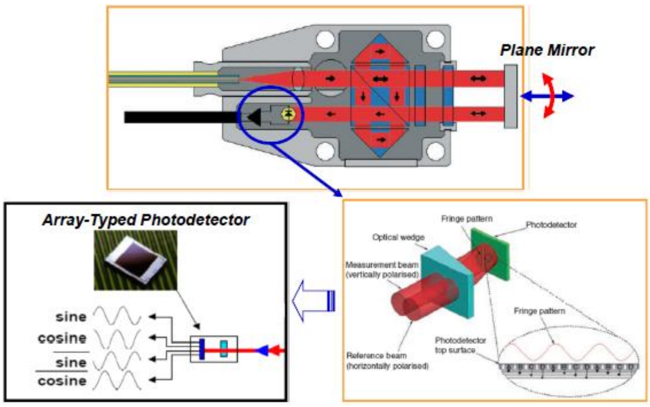

Fig.1 Homodyne differential plane mirror interferometer (HDPMI) (Renishaw RLD20 + RLD10-A3-P0)

As shown in Fig. 2, the low-noise DC power supply for the RLD10 detector unit, as recommended by the Renishaw's HDPMI expert, was exploited to minimise the electric noise components of the RLD10 analogue quadrature (cosine and sine) output signals as much as possible. Resultantly, the RLD10 photo detector is isolated from the electric noises of the DC power of the RLD20 unit that includes the electric noises of all the digital logics. The differential cosine and sine output signals of the RLD10 photo detector are converted to the single-ended cosine and sine signals (refer to the "DI-to-SE" converter in Fig. 2). The cosine and sine signals of dual DI-to-SE converters are connected to the input channels of the 12-bit digital oscilloscope (Lecroy HDO 6054) .

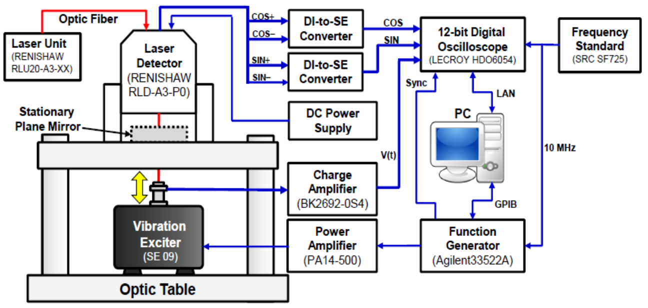

Fig. 2 Block diagram of new primary linear vibration calibration system under development in KRISS.

2.2 Displacement Measurement Principle

Let a time series of the cosine and sine outputs of the RLD10 detector unit (sampled by the *12-bit digital oscilloscope HDO 6054)* be $\{u_c(n)$ and $u_s(n)$: $n = 0, 1, 2, \cdots \}$. Both sampled signals are represented to be

$$u_c(n) = R\cos\left(8\pi\frac{d(n)}{\lambda}\right) + p \qquad (1)$$

$$u_s(n) = \frac{R}{r}\sin\left(8\pi\frac{d(n)}{\lambda} - \alpha\right) + q$$

Symbols in equation (1) are as follows: $d(n)$ = vibration displacement sample at time $t = n\cdot\Delta t$ (Δt = sampling interval), R = amplitude of photo detector signal, r = amplitude ratio of sine signal in reference to cosine signal, α = quadrature error angle, p and q = offset levels of cosine and sine (quadrature) signals, and λ = wavelength of a stabilized He-Ne laser. Heydemann [2] proposed the model of equation (1) in 1981 to measure the length of a sub-wavelength scale. He proposed the systematic way of evaluating the model parameters $\{R, r, \alpha, p, q\}$ using the least squares method [2]. Given the best-fitted model parameters, the corrected cosine and sine signals are obtained from the measured ones $\{u_c(n)$ and $u_s(n)$: $n = 0, 1, 2, \cdots\}$. Finally, a sampled time series of the corrected cosine and sine signals $c_c(n)$ and $c_s(n)$ are obtained as

$$c_c(n) = R\cos(\theta(n))$$

$$c_s(n) = R\sin(\theta(n)) \qquad (2)$$

Specifically, it will be demonstrated in the next section that this Heydemann correction scheme is significant in measuring the vibration displacement in the high frequency range of 5 kHz to 20 kHz (or higher).

In equation (2), the corrected cosine and sine components actually include electric noise components $n_c(n)$ and $n_s(n)$. Those noisy cosine and sine signals are used to estimate the phase angle $\theta(n)$ and then finally evaluate the vibration displacement $d(n)$,

$$\theta(n) = \arctan\left(\frac{R\sin(\theta(n)) + n_s(n)}{R\cos(\theta(n)) + n_c(n)}\right) \qquad (3)$$

$$d(n) = \frac{\lambda}{8\pi}\theta(n) \qquad (4)$$

2.3 'Zero Drift' Test Results

The first technical issue is to examine the "zero drift" characteristics of the new primary calibration system under development. This issue is to see what amount of the displacement the interferometer of interest provides when the target mirror is ideally stationary. A single and stationary common mirror that reflects both reference and measurement laser beams is configured to simulate an ideal zero displacement condition. Since the common mirror is stationary, the sine and cosine output signals of the RLD10 detector unit are frozen. The displacement model of equation (4) enables the evaluation of the displacement measurement uncertainty $u(d)$

$$u(d) = \frac{\lambda}{8\pi}\cdot\left\{\frac{m_s^2}{R^4}\sigma^2(c_c) + \frac{m_c^2}{R^4}\sigma^2(c_s) - 2\frac{m_c m_s}{R^4}\sigma^2(c_c, c_s)\right\}^{1/2} \qquad (5)$$

Note that the symbol symbols m_c and m_s in equation (6) denote the mean values of corrected cosine and sine signals, $\sigma^2(c_c)$, $\sigma^2(c_s)$, and $\sigma^2(c_c,c_s)$ their variance and covariance, and amplitude $R = \sqrt{m_c^2 + m_s^2}$. Fig. 3 illustrates the measurement noise models of sampled cosine and sine signals and their statistic properties.

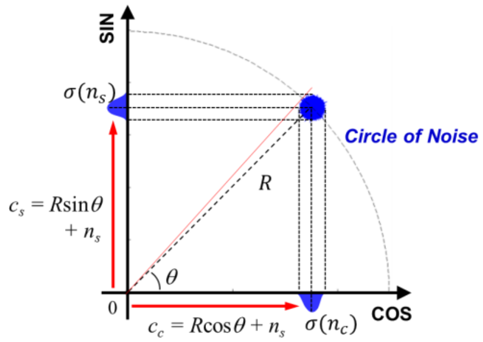

Fig. 3 Measurement noise models of sampled cosine and sine signals.

Fig. 4 illustrates the distributions of the measured noise components of the cosine and sine signals sampled at the rate of 10 MHz.

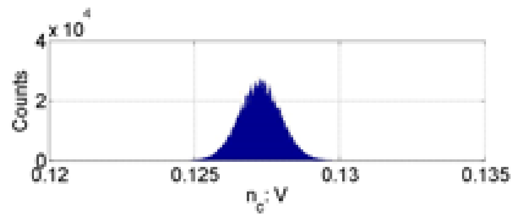

(a) Noise distribution of cosine signal

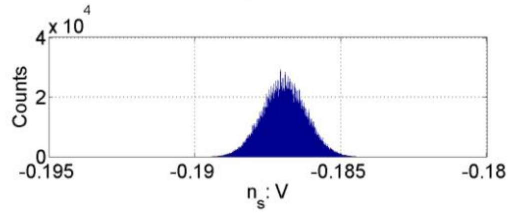

(b) Noise distribution of sine signal

Fig. 4 Distributions of measured cosine and sine signals.

Table 1 shows the statistical parameters of the filtered cosine and sine signals decimated by the ratio of 50 (i.e. sampling frequency = 200 kHz and displacement bandwidth = 100 kHz). The parameters in Table 1 indicate that the displacement measurement uncertainty approaches to 10.8

pm. It means that the new laser interferometer enables displacement measurement in a scale of 10 pico-meters.

Table 1. Electrical noise components of the cosine and sine signals measured form the stationary mirror.

m_c	m_s	$\sigma(c_c)$	$\sigma(c_s)$	$\sigma(c_c,c_s)$
122.9 mV	-180.6 mV	92.9 μV	82.8 μV	38.2 μV

Fig. 5 shows the linear spectral density over the frequency range of 10 Hz to 100 kHz. Four peak levels were observed to be 0.42 pm / $\sqrt{Hz}$ at 2.52 kHz, 0.67 pm / $\sqrt{Hz}$ at 5.05 kHz, 0.14 pm / $\sqrt{Hz}$ at 8.7 kHz, and 0.36 pm / $\sqrt{Hz}$ at 23 kHz. These results reveal that the new laser interferometer can unfold another possibility of realizing much improvement of vibration measurement uncertainty in the high frequency range of 5 kHz to 25 kHz.

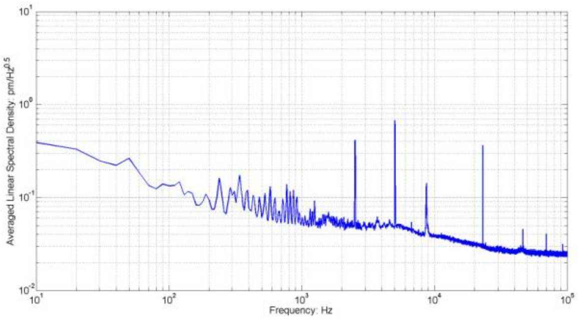

Fig. 5 Linear spectrum measured from the stationary target mirror.

3. PRIMARY LINEAR VIBRATION CALIBRATION SYSTEM UNDER DEVELOPMENT

3.1 Configuration of New Primary Calibration System

Fig. 6 shows the photo of a displacement measurement apparatus for the new primary linear vibration calibration system under development in KRISS. To generate the less harmonics and drift motion of the vibration table, the high-frequency vibration exciter (Spectra SE-09) [2] was also selected and installed on the vibration isolation table, as shown in Fig. 6.

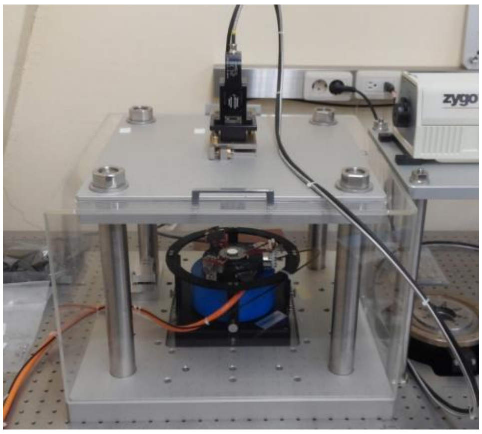

Fig. 6 Photo of the displacement measurement apparatus of a new primary linear vibration calibration system.

Previously shown in Fig. 2, the new primary calibration system does not only focus on the extension of the calibration frequency up to 20 kHz but also aims to includes the phase shift of the complex sensitivity as one of the new service items.

One of interesting features of the new calibration system is to use the frequency standard (Rubidium atomic clock SRC SF725) to provide the 10 MHz reference clock to the signal generator (Agilent 33522A), the digital oscilloscope (HDO 6054), and other instruments. Without using the common reference frequency source, the identical calibration frequency cannot be realized among the signal source, the digital scope and the frequency counter. Fig. 7 shows the moduli and phases of the accelerometer output signals of 20 kHz over the 10,000 periods when the internal clock source of the digital oscilloscope was set as in a normal mode. The noticeable drift of the phases shown in Fig. 7 seems to be a serious problem since it causes an unwanted bias of the averaged modulus and phase over the long periods.

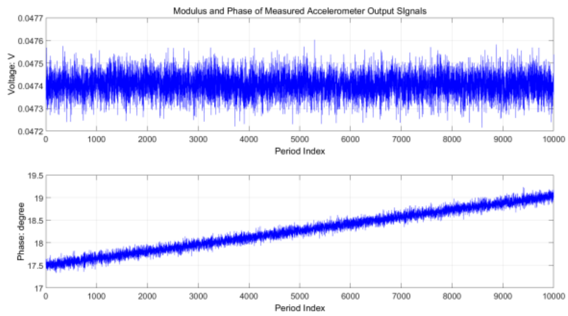

Fig. 7 Moduli and phases of the accelerometer output signal of 20 kHz recorded in 0.5 second (10,000 periods).

3.2 Vibration Measurement and Calibration Results

The calibration of accelerometers requires simultaneous measurements of the applied acceleration input and voltage output signals. As shown in Fig. 6, the HDPMI model is used to measure the displacement of the applied acceleration on the top table of the linear exciter. Table 2 illustrates the standard uncertainty of the measured vibration amplitude over the high frequency range of 5 kHz to 10 kHz.

Table 2. Standard measurement uncertainty of the modulus of the applied vibration displacement.

Frequency	Acceleration	Displacement	Standard uncertainty	
Hz	m/s^2-rms	nm	%	pm
5,000	168.1	240.9	0.096	231
10,000	63.93	22.90	0.107	24.5
20,000	50.50	4.52	0.142	6.4

As shown in Table 2, stable and of the measured vibration amplitude was close to 0.1 % at 5 kHz. As the frequency increased to 20 kHz it was shown to be close to 0.15 %. Although the standard uncertainty of the modulus of the accelerometer output signals is not shown in Table 2, it was found to be less than 0.02 % even in the high frequency range of 5 kHz to 20 kHz, which is a typical level achieved by advanced NMIs. The uncertainty of the measured vibration amplitude using the laser interferometer was found to be much higher than that of the modulus of the accelerometer output voltage signals.

Table 3. Complex sensitivity of an accelerometer evaluated at the four preferred frequencies.

Frequency	Complex Sensitivity				Standard Uncertainty	
	Real Part	Imag Part	Modulus	Phase	Modulus	Phase
	V/[m/s^2]		V/[m/s^2]	°	Relative	°
100 Hz	-1.064E-02	-7.702E-05	0.01064	180.41	0.009%	0.0008
5 kHz	-1.092E-02	2.846E-05	0.01092	179.85	0.21%	0.09
10 kHz	-1.099E-02	1.926E-04	0.01099	179.00	0.32%	0.44
20 kHz	-1.153E-02	3.887E-04	0.01154	178.07	0.46%	0.57

Table 3 lists the moduli and the phase shits of the complex sensitivity of an ICP-typed reference (working standard) accelerometer (imbedded inside the top table of the vibration exciter) and their corresponding measurement uncertainties. The modulus and the phase shift at each calibration frequency was evaluated by averaging the 12 moduli and phase shits measured at the four different alignment angles (0°,90°, 180°, and 270°) of the HDPMI head shown in Fig. 6. The standard uncertainties of the modulus are shown to increase noticeably, compared to the listed uncertainties in Table 2. One of main reasons is found to come from the four trials of the alignment angles of the HDPMI head for each 90°. This issue will be resolved by replacing the current alignment jig by a high precision one.

Another issue of the increased measurement uncertainty listed in Table 3 was found to come from the cosine and sine output signals of the RLD10 detector unit. Fig. 8 shows the Lissajous curve of the cosine and sine output signals recorded at the calibration frequency of 20 kHz. The blue one indicates the measured data and the red does the corrected one by using the Heydemann correction scheme [2]. The center of the blue curve is seen to be shifted from the origin. These shifted and elliptic (not circle) curve does not provide correct displacement data such that the modulus of the vibration displacement can be incorrect and distorted.

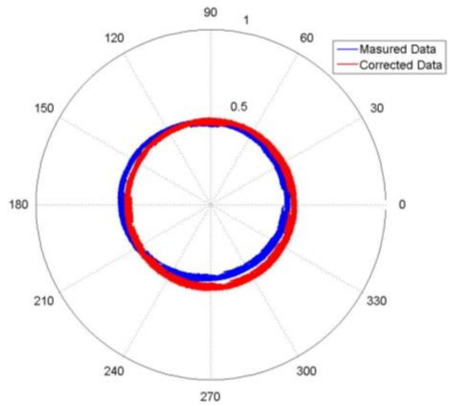

Fig. 8 Lissajous curve of the cosine and sine output signals of the RLD10 detector unit.

Table 4 lists the complex sensitivities measured from the four different alignment angles of the HDPMI head. The four bottom rows show the averaged values of the real and imaginary parts of the complex sensitivity, their modulus and phase, and their standard uncertainty. The Heydemann correction was shown to provide 0.65 % magnitude difference between both estimated moduli and 0.2° phase difference respectively.

Table 4. Listings of complex sensitivities measured at the calibration frequency of 20 kHz.

DPMI Head-Align Angle	Hydemann Correction Method			
	Not Applied		Applied (Corrected)	
	Complex Sensitivity		Complex Sensitivity	
	Real	Imag	Real	Imag
	V/(m/s^2)	V/(m/s2)	V/(m/s2)	V/(m/s2)
0°	-1.176E-02	1.676E-04	-1.167.E-02	2.040.E-04
	-1.172E-02	-6.495E-05	-1.160.E-02	-3.220.E-05
90°	-1.154E-02	2.275E-04	-1.152.E-02	2.628.E-04
	-1.138E-02	9.662E-04	-1.126.E-02	9.869.E-04
180°	-1.166E-02	2.771E-04	-1.152.E-02	3.058.E-04
	-1.152E-02	5.779E-04	-1.141.E-02	6.052.E-04
270°	-1.160E-02	6.076E-04	-1.154.E-02	6.394.E-04
	-1.164E-02	9.621E-05	-1.170.E-02	1.376.E-04
Mean	-1.160.E-02	3.569.E-04	-1.153.E-02	3.887.E-04
Modulus	0.01161 V/(m/s2)		0.01153 V/(m/s2)	
Phase	178.24°		178.07°	
Std. Un.	0.39%	0.58°	0.46%	0.57°

4. CONCLUDING REMARKS

A homodyne differential plane mirror interferometer (HDPMI) model is chosen to develop a next generation model for the primary linear vibration calibration system in KRISS. Its zero-drift test results showed that displacement measurement in a scale of 10 pico-meters could be feasible. It may indicate that the HDPMI could be quite successful for the primary vibration calibration even in the frequency range of 5 kHz to 20 kHz.

The classical Heydemann model was exploited to estimate the five parameters of the cosine and sine signals of the HDPMI optic detector. Specifically, the corrected cosine and sine signals were shown to be significant in vibration measurement in the high frequency range of 5 kHz to 20 kHz. The standard uncertainty of the complex sensitivities in the range of 5 kHz to 20 kHz was shown to be less than 0.5 % for their moduli and 0.6° for the phase shifts, respectively.

5. ACKNOWLEDGEMENTS

This research was partially supported by NRF (National Research Foundation of Korea) and KRISS (NRF project code = 201R1A2A1A11050897, KRISS project number = 17011120)

6. REFERENCES

[1] Wan-Sup Cheung and Kyungmin Baik, “Challenges for High-Frequency primary Calibration of Vibration: Pico-meter Metrology,” *inter-noise 2015,* San Francisco: USA, August 2015.

[2] Holger Nicklich and Martin Brucke, “Latest Design of Sine and Shock Exciters for Calibration Purposes,” *IMEKO-TC22 International Conference,* Merida: Mexico, November 2007

[3] P. L. M. Heydemann, “Determination and correction of quadrature fringe measurement errors in interferometers,” *Appl. Opt.* 20(19),(1981).